Journal of Medical Imaging & Case Reports

https://doi.org/10.17756/micr.2018-004

Research Article

Open Access

Prospective Assessment of Variability and Reproducibility of Diffusion-Weighted MRI and T2-Mapping of the Pancreas in Healthy Volunteers

Jaymin Upadhyay[1*], Sev Dolgopolov[2], Jayant Narang[2], Christine Millet[2], Rinal Patel[1], Dinko Gonzalez-Trotter[1] and Edward Ashton[2]

[1]Regeneron Pharmaceuticals, Tarrytown, NY, USA
[2]BioTelemetry Research, Rochester, NY, USA

[*]Correspondence to:
Jaymin Upadhyay, PhD
777 Old Saw Mill River Road
Regeneron Pharmaceuticals
Tarrytown, NY, 10591, USA
Tel: (914) 336-0769
E-mail: Jaymin.Upadhyay@regeneron.com

Received: September 11, 2017
Accepted: January 31, 2018
Published: February 03, 2018

Citation: Upadhyay J, Dolgopolov S, Narang J, Millet C, Patel R, et al. 2018. Prospective Assessment of Variability and Reproducibility of Diffusion-Weighted MRI and T2-Mapping of the Pancreas in Healthy Volunteers. *J Med Imaging Case Rep* 1(1): 16-23.

Published by United Scientific Group

Abstract

Purpose: To determine the test-retest reliability and variance of metrics obtained from pancreatic diffusion-weighted magnetic resonance imaging (DW-MRI) and T2-MRI (i.e., apparent diffusion coefficients (ADC) and T2-relaxation times).

Methods: A two scanning session, two observer test-retest study in healthy volunteers (N=10) at 1.5T was performed with DW-MRI and T2-mapping scans acquired. In addition to region-specific (head, neck, body and tail) ADC and T2-relaxation values, coefficients of variation (CVs) and Bland-Altman plots were calculated.

Results: We observed mean ADC values (x 10^{-3} mm^2/sec) of head: 1.50 - 1.56, neck: 1.38 - 1.61, body: 1.32 - 1.37 and tail: 1.19 - 1.20. The mean T2-relaxation times (msecs) were head: 60.23 - 63.14, neck: 57.80 - 58.63, body: 58.78 - 59.69 and tail: 58.82 - 59.99. Based on CVs, lower inter-scan session and inter-observer variability were consistently calculated for T2-relaxation times (CV of ~4%) compared to ADCs (CV of ~18%). Bland-Altman analyses did not reveal any systematic trends in bias.

Conclusions: Given the superior test-retest reliability observed for T2-mapping over DW-MRI, T2-mapping may enable more sensitive pancreatic lesion detection and monitoring. The current set of results can aid the study design of future longitudinal clinical trials, aiming to track the evolution or resolution of pancreatic pathology with DW-MRI or T2-mapping methodologies.

Key Words

Pancreas, Test-retest reliability, DW-MRI, T2-mapping, Coefficient of variation

Introduction

In conditions such as acute pancreatitis, contrast-enhanced computed tomography (CT) is considered the primary imaging modality for revealing pancreatic disease severity, monitoring treatment response or providing diagnostic clarity [1, 2]. However, in patients for whom contrast-enhanced CT is contraindicated, magnetic resonance imaging (MRI) is a recommended and frequently utilized alternative to assessing pancreatic health. For longitudinal investigation of the diseased pancreas, where multiple imaging evaluations are needed within a short timeframe, MRI has the added value over CT given the lack of substantial radiation exposure or need for exogenous contrast agents that enable identification of pancreatic pathology. To date, MRI methods, mainly

diffusion-weighted MRI (DW-MRI) and T2-MRI, have shown sensitivity for detecting pathology in acute or chronic pancreatitis [3-7], autoimmune pancreatitis [8-10] and pancreatic cancer [11-13].

During early stages of pancreatic injury or inflammation, acinar cell injury, activation of pancreatic stellate cells and an invasion by leukocytes, neutrophils and macrophages are all known to exist [14]. Such intracellular, extracellular and intravascular pathological events modulate microstructural properties of affected pancreatic tissue, and in turn, alter the random Brownian motion of water molecules in each biological compartment. From DW-MRI experiments aimed at measuring apparent diffusion coefficients (ADCs), it is known that inflammatory compared to healthy pancreatic tissue is characterized as having restricted water diffusion (decreased ADCs), while less restricted water diffusion (increased ADCs) occurs in necrotic lesions [3, 11]. With respect to T2-MRI signals, presence of inflammatory infiltrates and parenchymal changes can be identified by regions of increased T2-weighted signal intensities or prolonged T2-relaxation times [5].

A substantial number of studies have independently demonstrated the utility of DW-MRI and T2-MRI for quantifying focal and diffuse lesions in various patient populations possessing compromised pancreatic function and structure. From this body of work, a better working understanding of optimal image acquisition and analysis parameters for pancreatic MRI studies is in place [15]. One methodological aspect in need of further inquiry pertains to the inter- scan session and inter-observer, test-retest reliability of DW-MRI and T2-MRI. Thus far, a limited number of investigations have reported on this topic [16-19]. Therefore, we aimed to perform a test-retest study in healthy volunteers and compare the variability and reproducibility of metrics obtained from DW-MRI (ADC) and T2-mapping (T2-relaxation times) across 4 pancreatic regions (head, neck, body and tail). Using the results presented herein, guidance on methodological limitations, study design parameters and appropriate powering of study endpoints can be obtained for future DW-MRI or T2-mapping investigations, where the goal is to monitor pancreatic pathology or a novel therapy that is hypothesized to mediate pancreatic disease states.

Materials and Methods

Healthy volunteers

Pancreatic MRI data was collected in ten healthy volunteers (9 females, 1 male, aged 22-68 years). Institutional Review Board approval was obtained prior to the study, and all subjects gave informed consent to participate.

MRI data acquisition

Subjects were scanned in the supine position. Images of the abdominal region including the pancreas were obtained using respiratory gating and fat saturation. Positioning was identical for DW-MRI and T2-mapping scans. Each subject underwent two scanning session in a single day, where the delay between repeated scans ranged from 30-60 mins. The MRI protocol included a three-plane localizer, axial and coronal T2-weighted MRI, DW-MRI and T2-mapping scans. All data were collected using a 1.5T Siemens Aera system (Erlangen, Germany) and phased array torso coil enable full coverage of the pancreas (Figure 1A). This study was performed at 1.5T given the substantial body of prior pancreatic MRI investigations performed at this field strength, which the current set of results could be compared to, as well as guidance around MRI protocol optimization at 1.5T [15].

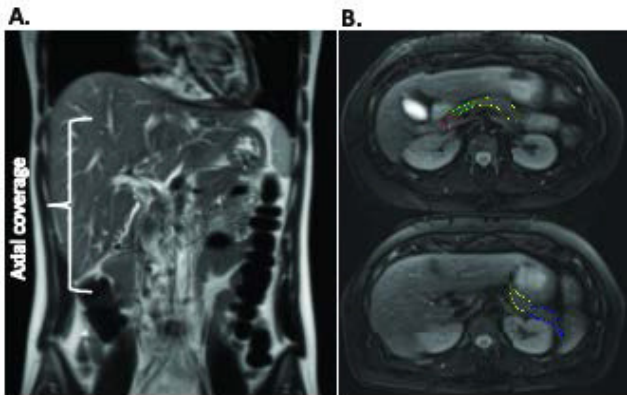

Figure 1: A) A coronal Half-Fourier Acquisition Single-shot Turbo Spin Echo Image (HASTE) image showing positioning of axial slice position for subsequent DW-MRI and T2-mapping MRI. **B)** Pancreatic sub-regions (head: red, neck: green, body: yellow and tail: blue) were manually segmented for each subject. A single-subject, single observer example is shown here.

DW-MRI parameters: Pulse Sequence = Echo Planar Imaging Spin-Echo, TR/TE = 5000/68 msecs, matrix = 134x134, Slice Thickness = 6 mm with 20% slice gap, NSA = 1, Bandwidth 2332 Hz/Px, Diffusion Directions = 3 (orthogonal weighting), b-values = 0, 150, 450 and 900 secs/mm^2 and Scan Time = 2 mins.

T2-Mapping parameters: Pulse Sequence = Spin Echo, TE = 6 echos (15-90 msecs), TR = 1800 msecs, matrix = 192x192, Slice Thickness = 6 mm with 20% slice gap, # of averages = 3, Bandwidth 130 Hz/Px and Scan Time = 8 mins. Both DWI and T2-mapping were acquired with 40 cm FOV and 70% phase resolution.

Data analysis

Pancreatic sub-regions (head, neck, body and tail) were identified for each subject and visit manually via tracing with a computer mouse by two radiologists using custom, in-house image analysis software (BioTelemetry Research, Rochester, NY, USA) (Figure 1B). Tracing was performed independently on DW-MRI and T2-mapping data, with each radiologist blinded to the other's results and scan session. Readers had access to all acquired b-values during the DWI analysis and to all echoes during the T2-mapping analysis and were able to see how the applied contours fit to each image. Readers were instructed to include the maximum practical portion of the organ, while excluding regions of clear partial volume effects. ADC and T2-relaxation times were calculated at each pixel in the images, as described below. Mean values for each parameter were then generated from the set of pixels fully

contained within the boundaries for each of the four pancreatic sub-regions. A total of twelve diffusion images were acquired at each location: three directions (x, y, z) and four b-values (0, 150, 450, and 900 secs/mm^2). This allowed for the calculation of nine diffusion coefficients $D_{x,i}$, given by:

$$D_{x,i} = \ln[S(b_0)/S(b_i)]/b_i, \quad \text{..... (1)}$$

where $S(b_i)$ is the observed signal at b-value i. The ADC at each pixel was then given by the arithmetic mean of the nine calculated diffusion coefficients.

In a T2-weighted image, the signal intensity, S, can be represented as a constant B times an exponential decay, as:

$$S = Be^{-\frac{TE}{T_2}} \quad \text{..... (2)}$$

where TE is the echo time. Taking the natural log of the signal yields:

$$\ln(S) = \ln(B) - \frac{TE}{T_2} \quad \text{..... (3)}$$

The resulting equation is a line with slope of -1/T2. To estimate the value of T2, a linear regression is performed on the natural log of the signal intensities:

$$T_2 = \frac{\sum TE_n^2 - \frac{1}{N}\sum TE_n \sum TE_n}{\sum TE_n \ln(S_n) - \frac{1}{N}\sum TE_n \sum \ln(S_n)} \quad \text{..... (4)}$$

where TE_n is the echo time of the nth echo, S_n is the signal intensity of the nth echo, and N is the number of echoes. Note that while T2-relaxation times can be estimated from as few as two echoes, more echoes will provide a better estimate of the slope in the presence of noise [20]. Selection of echo times is constrained by two factors: greater time between echoes minimizes the effect that noise will have on the estimated slope. However, if the echo time becomes too large, the signal will be dominated by noise for short T2-decay times. The set of echo times selected for this study, ranging from 15 mecs – 90 mecs, was intended to optimize the tradeoff between these two constraints.

Statistical analysis

In order to identify statistically significant inter-scan session and inter-observer differences, two-tailed, paired t-tests were utilized. Variability and reproducibility of regional ADCs and T2-relaxation times were obtained by calculating the coefficients of variation (CV) and using the Bland-Altman analysis method (GraphPad Prism 6.0), where the bias and 95% confidence interval of the mean absolute difference (i.e., Scan session 1 – Scan session 2 and Observer 1 – Observer 2) were obtained. A two-tailed, Mann-Whitney U test was used to test for significant differences in CVs between ADCs and T2-relaxation for each pancreatic sub-region and each observer.

Results

Upon visual inspection, T2-mapping data at each echo enabled clear delination of the pancreas as well as other abdominal structures with little to no image artifact present (Figure 2). As expected, DW-MRI data qualitatively showed poorer image quality compared to T2-maps, particularly at the higher b-values (Figure 3). However, no trends in DW-MRI data quality were observed with respect to diffusion direction. All DW-MRI and T2-mapping datasets were judged by both blinded observers as possessing sufficient data quality and subsequently quantified.

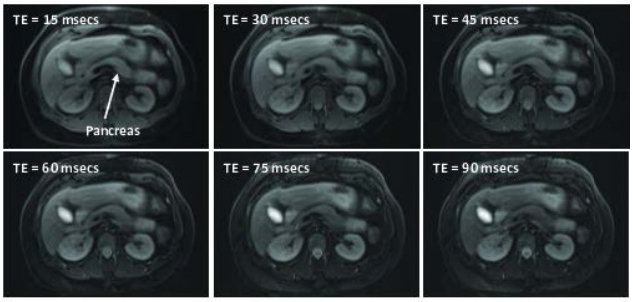

Figure 2: Axial images depicting the pancreas and acquired from T2-mapping are shown for a single, representative healthy volunteer. Data is shown for each echo time utilized in the current investigation.

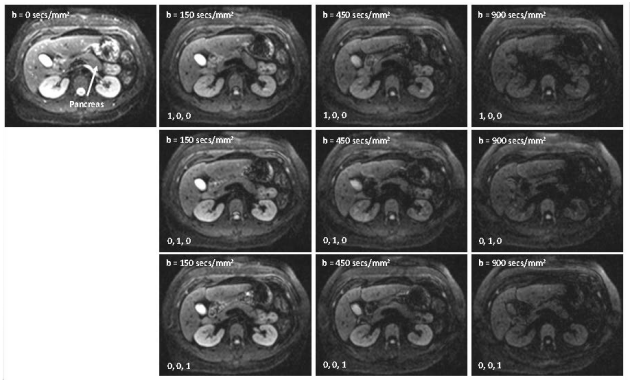

Figure 3: Axial images depicting the pancreas and acquired from DW-MRI are shown for a single, representative healthy volunteer. The corresponding T2-mapping data for this subject is shown in figure 2. Axial diffusion-weighted images are shown for each b-value as well as each diffusion direction utilized in the current investigation.

Across the 4 pancreatic sub-regions, 2 scan sessions and 2 observers, ADCs and T2 relaxation times ranged from 1.19 - 1.61 x 10^{-3} mm^2/secs and 57.80 - 63.14 msecs, respectively (Table 1). A significant (uncorrected for multiple comparisons, p = 0.04) inter-scan session difference was solely observed for mean ADC values for observer 2 in the neck region. Significant inter-scan session differences for T2-relaxation were not present.

Inter-scan session and inter-observer CVs for ADCs as well as T2 relaxation times are given in table 2. Independent of the pancreatic sub-region, test-retest ADC variability was consistently and substantially higher compared to variability measured for T2-relaxation times. The neck region ADCs possessed particularly high ranges of variability for both observers. Inter-observer CVs were comparable and of low magnitude for either metric.

Table 1: A) Mean pancreatic ADC across sub-regions and observers. **B)** Mean pancreatic T2-relaxation times across sub-regions and observers

A)

ADC	(mean ± SD) x 10^{-3} mm^2/sec Scan Session 1	(mean ± SD) x 10^{-3} mm^2/sec Scan Session 2
Head		
Observer 1	1.50 ± 0.28	1.53 ± 0.30
Observer 2	1.50 ± 0.33	1.56 ± 0.29
Neck		
Observer 1	1.42 ± 0.30	1.57 ± 0.33
Observer 2	1.38 ± 0.31	1.61 ± 0.32*
Body		
Observer 1	1.32 ± 0.32	1.37 ± 0.20
Observer 2	1.33 ± 0.32	1.32 ± 0.20
Tail		
Observer 1	1.19 ± 0.28	1.20 ± 0.24
Observer 2	1.19 ± 0.20	1.20 ± 0.19

B)

T2 Relaxation Times	(mean ± SD) msecs Scan Session 1	(mean ± SD) msecs Scan Session 2
Head		
Observer 1	60.93 ± 6.55	60.35 ± 4.65
Observer 2	60.23 ± 3.82	63.14 ± 7.01
Neck		
Observer 1	58.38 ± 3.38	57.80± 5.75
Observer 2	58.12 ± 4.06	58.63 ± 4.75
Body		
Observer 1	58.98 ± 4.55	59.85 ± 6.80
Observer 2	59.69 ± 5.42	58.78 ± 5.28
Tail		
Observer 1	58.94 ± 2.92	58.94 ± 3.80
Observer 2	58.82 ± 4.40	59.99 ± 4.25

*$p < 0.05$

were not found for either MRI metric or for any pancreatic sub-region. Neck region ADCs did show a greater magnitude of bias compared to the head, body and tail. With exception to the neck region ADCs, the magnitude of bias as a percentage of the mean was comparable between ADCs and T2-relaxation times.

Discussion

Several useful observations can be made based on the data presented above. First and most obviously, a T2-MRI based assessment is significantly less variable between scan sessions and observers than DW-MRI. This should not strictly mean that T2-MRI necessarily provides a more useful target in any given clinical situation, however, as the critical metric in this case is the ratio of the variability to the magnitude of change expected due to either disease progression or response to treatment. It is also interesting to note that the inter-observer coefficient of variation for ADC assessment across all regions was roughly one third of the inter-scan CV. This indicates majority of the variability seen in this measure is the result not of observer error, but rather of differences in the scans. This was not true for T2-mapping, where inter-observer variability was similar to inter-scan variability. The latter observation reinforces the fact that pancreatic ADCs were inherently more variable than T2-relaxation times.

The region-specific, ADCs reported herein for healthy pancreatic tissue agree with past investigations [6, 16, 18, 19, 21-23]. In a recent review by Barral et al., the mean ADC across numerous studies and normal pancreatic head, neck, body and tail were 1.52, 1.27, 1.48, and 1.36 x 10^{-3} mm^2/secs, respectively [15]. An insignificant trend towards decreasing ADCs from the head to tail regions, is also commonly observed amongst the current and previous DW-MRI studies

Table 2: Coefficients of variations (%) for ADC and T2-relaxation times

	Coefficients of Variation (95% CI) Inter-Scan Session (ADC)	Coefficients of Variation (95% CI) Inter-Scan Session (T2-Relaxation Times)	p-value	Coefficients of Variation (95% CI) Inter-Observer (ADC)	Coefficients of Variation (95% CI) Inter-Observer (T2-Relaxation Times)
Head					
Observer 1	11.29 (6.68 - 15.90)	4.75 (0.77 - 8.73)	0.009	5.15 (2.63 - 7.67)	4.46 (2.09 - 6.83)
Observer 2	17.23 (9.70 - 24.76)	4.49 (0.59 - 8.39)	0.005		
Neck					
Observer 1	24.57 (9.28 - 39.86)	5.10 (2.72- 7.48)	0.002	8.63 (5.24 - 12.02)	2.55 (1.61 - 3.50)
Observer 2	19.08 (7.13 - 31.03)	3.62 (1.93 - 5.31)	0.05		
Body					
Observer 1	16.10 (4.05 - 28.15)	3.51 (1.34 - 5.69)	0.007	4.92 (1.24 - 8.60)	1.75 (0.87 - 2.63)
Observer 2	19.98 (7.38 - 32.58)	2.64 (1.87 - 3.41)	0.001		
Tail					
Observer 1	18.56 (7.55 - 29.57)	2.47 (1.29 - 3.65)	0.0002	6.81 (3.56 - 10.06)	3.85 (2.51 - 5.19)
Observer 2	13.91 (5.81 - 22.01)	4.55 (1.86 - 7.24)	0.04		

Bland-Altman plots were assessed for ADCs (Figure 4) and T2-relaxation times (Figure 5). Significant positive or negative correlations between mean differences and averages [6, 19, 21]. From a microstructural perspective, a healthy pancreas may be considered homogeneous in comparison to other organs such as the brain. However, prior investigations

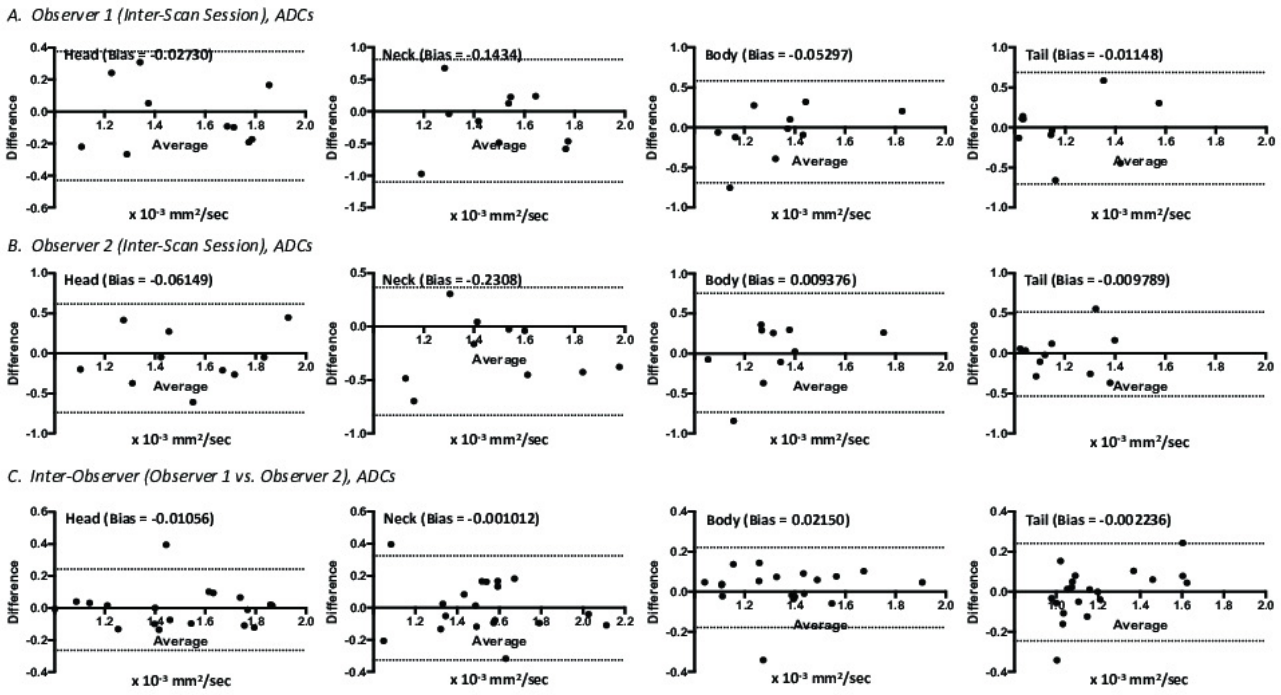

Figure 4: Bland-Altman plots for ADCs for each pancreatic sub-region. Plots were individually derived for Observer 1 **(A.)** and Observer 2 **(B.)**, where values from scan sessions 1 and 2 were averaged. For inter-observer Bland-Altman plots, ADC values were averaged between the two observers **(C.)**.

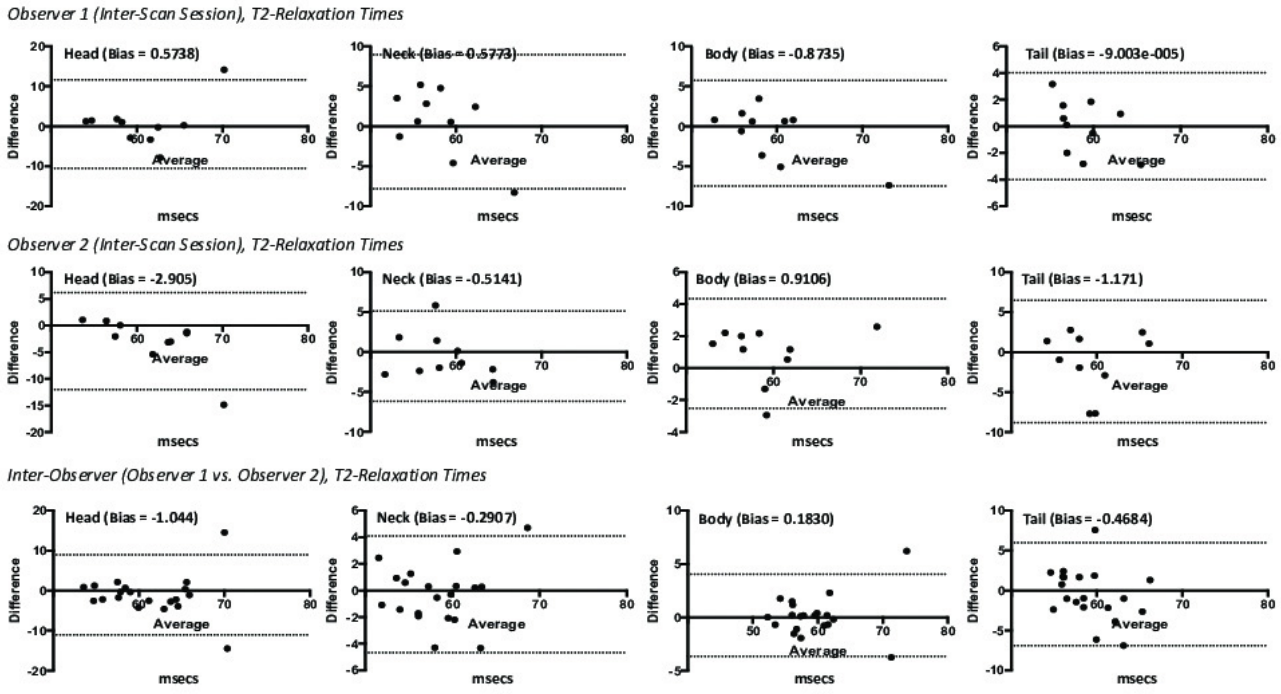

Figure 5: Bland-Altman plots for T2-relaxation times for each pancreatic sub-region. Plots were individually derived for Observer 1 **(A.)** and Observer 2 **(B.)**, where values from scan sessions 1 and 2 were averaged. For inter-observer Bland-Altman plots, T2 relaxation times were averaged between the two observers **(C.)**.

have reported biological differences between pancreatic regions, where age, gender and fat content may contribute to heterogeneous ADCs reported either between studies or between pancreatic sub-regions [24, 25]. Nonetheless, inter-regional variability in ADCs may stem from technical reasons and requires further investigation (potential factors contributing DW-MRI variability in the pancreas are discussed below). What between-study differences in ADCs

are present likely arise from the wide range of data acquisition and analysis procedures implemented. For example, while more than two b-values were utilized in some studies [3, 16], including the current one, others estimated ADCs using just 2 b-values (e.g., 0 and 800 secs/mm^2) [19, 22]. The presence of intravoxel incoherent motion in DW-MRI data and how this effect was or was not accounted may have also influenced computed ADC values, particularly when low b-values were utilized [26]. Other procedural anomalies contributing to between-study ADC variability include but are not limited to implementation of breath-hold, triggering methodology, use of 1.5T or 3T scanners, landmarks used to segment pancreatic sub-regions or how ADCs are calculated (e.g., mono- vs. bi-exponential modeling). Pancreatic T2-relaxation times in this study fell within a range of 57.80 - 63.14 msec. By comparison, de Bazelaire et al. and Hoad et al., measured lower mean T2 relaxation times in normal pancreas to be 42 ± 20 (@ 3T), 43 ± 7 (@ 3T) and 46 ± 6 (@ 1.5T) msecs [27, 28]. Similar to DW-MRI studies, inter-study differences in T2-mapping acquisition parameters also exist. For example, here a multi-slice acquisition was used to cover the entire pancreas, whereas Hoad et al., sampled the pancreas with a single 10 mm coronal slice. Moreover, the implemented echo time range was also variable across investigations.

With exception to the neck region ADCs for observer 2, significant inter-scan session differences were not detected for either ADC or T2 relaxation times. Significant inter-observer differences for either metrics were undetected. Across the two observers and 4 pancreatic sub-regions, a mean CV of ~18% was calculated, which is similar to abdominal, DW-MRI investigations by Braithwaite et al. and Rosenkranz et al. By comparison, the mean CV for T2 relaxation times was substantially lower at ~4%, suggesting that detection of treatment effect may be more viable with T2-mapping than DW-MRI. However, whether DW-MRI or T2 mapping is more sensitive towards detecting pancreatic tissue pathology or treatment response is projected to also depend upon the disease state or stage affecting pancreatic microstructure, type of tissue pathology (e.g., edema, inflammation, hemorrhage, fibrosis and necrosis) or therapeutic strategy.

Test-retest reliability was evaluated by calculating inter-scan session and inter-observer Bland-Altman analyses. These analyses demonstrated that the inter-scan session mean bias (in units of 10^{-3} mm^2/secs) for ADCs and for both observers was of lower magnitude (range: -0.062 - 0.00094) for the head, body and tail compared to the neck (range: -0.23 - -0.14). Prior pancreatic, DW-MRI work performed at 1.5 T, show a bias (in units of 10^{-3} mm^2/secs) for ADCs of -0.04 - 0.04 [19] or 0.003 - 0.029 [16]. In agreement with the current study, Barral et al., reported 95% limits of agreement at 27% for the neck region, which was higher compared to other regions of the pancreas (< 11%). The smaller range in mean bias as well as the higher ADC values reported by Ye et al., are likely reflective of neck region ADCs not being quantified and implementation of 2 b-values (i.e., 0 and 600 secs/mm^2) to estimate pancreatic diffusion properties. Inter-observer ADC variability as quantified by the mean bias was commonly low across current and past studies. A similar trend in inter-scan session bias was not observed for T2-relaxation times, where the neck region of the pancreas demonstrated higher variability. This may suggest that the pancreatic neck is particularly prone to raw signal abnormalities that subsequently contribute to the higher level of ADC variability. The magnitude of the bias relative to the mean T2 relaxation times was also lower at ~5% compared to ~18% for ADC. Moreover, for either ADCs or T2 relaxation times, trends between mean differences and averages were not present.

Comparing T2-mapping and DW-MRI images (Figure 2 and 3), the latter show a higher level of image distortion within the pancreas and most notably when greater diffusion weighting was applied. While a single source could not be attributed for the poorer image quality observed for DW-MRI data and in turn, susceptibility to inter-scan variability, we hypothesized the presence of multiple contributing factors. Of these, the high sensitivity to patient motion, including respiratory movement (even in respiratory-gated, DW-MRI data), was considered a primary source of variability. Moreover, signal loss due to the presence of various tissue interfaces or partial volume effects likely confounded image quality and diminished test-retest reliability. To further minimize confounds stemming from partial volume effects specifically, acquisition of thinner slices or acquisition of slices in sagittal or coronal orientations may be considered in future investigations. Quantification of ADCs and T2-relaxation times using smaller regions of interest (ROI) should also be considered in order to better avoid partial volume effects. However, use of clear anatomical boarders delineating the pancreas or pancreatic sub-regions is considered pivotal for standardizing ROIs across time points or between observers.

A limitation of this study relates to physiological differences between the healthy volunteer population investigated herein compared to patient population suffering from pancreatic pathology, where MRI-based assessments have been or would be applicable. For example, acute pancreatitis patients are often comorbid with conditions such as obesity [29]. The presence of visceral fat, specifically pancreatic adipose tissue, can affect DW-MRI signal despite the application of fat suppression techniques. Such a disparity may yield increased variability to MRI measures not present within a healthy volunteer population. Additionally, the time interval between two adjacent imaging evaluations of the pancreas may differ between an investigation involving patients and healthy volunteer studies. In the former case, execution of MRI would primarily be dictated by the need for diagnostic clarity in response to a medical event or monitoring of a potential treatment response, in which case, the inter-scan interval would be longer compared to the current study. A longer inter-scan interval may yield a different level of variably and reproducibility than that elucidate in our study. Therefore, subsequent work, which builds off the current dataset, should indeed involve the longitudinal evaluation of patients with pancreatic disease (e.g., patients with acute pancreatitis). Such investigations would further enable a determination of the utility of pancreatic MRI towards monitoring pancreatic pathology and potential treatment effect. Lastly, recent retrospective work has suggested that conventional

metrics such as the mean ADCs of the pancreas may not be as sensitive towards monitoring pancreatic pathology or treatment response as other diffusion MRI measures [4, 30, 31]. Therefore, the variability and reproducibility of these novel approaches may be beneficial to consider.

Conclusions

In conclusion, this healthy volunteer study revealed better inter-scan session variability and reproducibility for T2 -mapping than DW-MRI across 4 pancreatic sub-regions. Inter-observer variability and reproducibility was comparable between the two MRI approaches. The results of this work can further aid the study design of future DW-MRI and T2-mapping studies aiming to longitudinally assess pancreatic injury or treatment effect on pancreatic injury using an MRI-based approach.

Conflict of Interest

Jaymin Upadhyay, Rinal Patel, and Dinko Gonzalez-Trotter are employees of Regeneron Pharmaceuticals. Sev Dolgopolov, Jayant Narang, Christine Millet and Edward Ashton are employees of BioTelemetry Research.

Acknowledgments

The authors would like to thank Travis Stoud, Allen Radin and Bachir Taouli for their input during the execution of this work.

Funding Source

This study was funded by Regeneron Pharmaceuticals.

References

1. Banks PA, Bollen TL, Dervenis C, Gooszen HG, Johnson CD, et al. 2013. Classification of acute pancreatitis--2012: revision of the Atlanta classification and definitions by international consensus. *Gut* 62(1): 102-111. https://doi.org/10.1136/gutjnl-2012-302779
2. Thoeni RF. 2012. The revised Atlanta classification of acute pancreatitis: its importance for the radiologist and its effect on treatment. *Radiology* 262(3): 751-764. https://doi.org/10.1148/radiol.11110947
3. de Freitas Tertulino F, Schraibman V, Ardengh JC, do Espírito-Santo DC, Ajzen SA, et al. 2015. Diffusion-weighted magnetic resonance imaging indicates the severity of acute pancreatitis. *Abdom Imaging* 40(2): 265-271. https://doi.org/10.1007/s00261-014-0205-y
4. Iranmahboob AK, Kierans AS, Huang C, Ream JM, Rosenkrantz AB. 2017. Preliminary investigation of whole-pancreas 3D histogram ADC metrics for predicting progression of acute pancreatitis. *Clin Imaging* 42: 172-177. https://doi.org/10.1016/j.clinimag.2016.12.007
5. Tang MY, Chen TW, Huang XH, Li XH, Wang SY. 2016. Acute pancreatitis with gradient echo T2*-weighted magnetic resonance imaging. *Quant Imaging Med Surg* 6(2): 157-167. https://doi.org/10.21037/qims.2016.04.03
6. Thomas S, Kayhan A, Lakadamyali H, Oto A. 2012. Diffusion MRI of acute pancreatitis and comparison with normal individuals using ADC values. *Emerg Radiol* 19(1): 5-9. https://doi.org/10.1007/s10140-011-0983-2
7. Xiao B, Zhang XM, Tang W, Zeng NL, Zhai ZH. 2010. Magnetic resonance imaging for local complications of acute pancreatitis: a pictorial review. *World J Gastroenterol* 16(22): 2735-2742. https://doi.org/10.3748/wjg.v16.i22.2735
8. Crosara S, D'Onofrio M, De Robertis R, Demozzi E, Canestrini S, et al. 2014. Autoimmune pancreatitis: multimodality non-invasive imaging diagnosis. *World J Gastroenterol* 20(45): 16881-16890. https://doi.org/10.3748/wjg.v20.i45.16881
9. Klauss M, Maier-Hein K, Tjaden C, Hackert T, Grenacher L, et al. 2016. IVIM DW-MRI of autoimmune pancreatitis: therapy monitoring and differentiation from pancreatic cancer. *Eur Radiol* 26(7): 2099-2106. https://doi.org/10.1007/s00330-015-4041-4
10. Negrelli R, Manfredi R, Pedrinolla B, Boninsegna E, Ventriglia A, et al. 2015. Pancreatic duct abnormalities in focal autoimmune pancreatitis: MR/MRCP imaging findings. *Eur Radiol* 25(2): 359-367. https://doi.org/10.1007/s00330-014-3371-y
11. Hayano K, Miura F, Wada K, Suzuki K, Takeshita K, et al. 2016. Diffusion-weighted MR imaging of pancreatic cancer and inflammation: Prognostic significance of pancreatic inflammation in pancreatic cancer patients. *Pancreatology* 16(1): 121-126. https://doi.org/10.1016/j.pan.2015.10.004
12. Kurosawa J, Tawada K, Mikata R, Ishihara T, Tsuyuguchi T, et al. 2015. Prognostic relevance of apparent diffusion coefficient obtained by diffusion-weighted MRI in pancreatic cancer. *J Magn Reson Imaging* 42(6): 1532-1537. https://doi.org/10.1002/jmri.24939
13. Pozzi-Mucelli RM, Rinta-Kiikka I, Wünsche K, Laukkarinen J, Labori KJ, et al. 2017. Pancreatic MRI for the surveillance of cystic neoplasms: comparison of a short with a comprehensive imaging protocol. *Eur Radiol* 27(1): 41-50. https://doi.org/10.1007/s00330-016-4377-4
14. Yadav D, Whitcomb DC. 2010. The role of alcohol and smoking in pancreatitis. *Nat Rev Gastroenterol Hepatol* 7(3): 131-145. https://doi.org/10.1038/nrgastro.2010.6
15. Barral M, Taouli B, Guiu B, Koh DM, Luciani A, et al. 2015. Diffusion-weighted MR imaging of the pancreas: current status and recommendations. *Radiology* 274(1): 45-63. https://doi.org/10.1148/radiol.14130778
16. Barral M, Soyer P, Ben Hassen W, Gayat E, Aout M, et al. 2013. Diffusion-weighted MR imaging of the normal pancreas: reproducibility and variations of apparent diffusion coefficient measurement at 1.5- and 3.0-Tesla. *Diagn Interv Imaging* 94(4): 418-427. https://doi.org/10.1016/j.diii.2012.12.007
17. Braithwaite AC, Dale BM, Boll DT, Merkle EM. 2009. Short- and midterm reproducibility of apparent diffusion coefficient measurements at 3.0-T diffusion-weighted imaging of the abdomen. *Radiology* 250(2): 459-465. https://doi.org/10.1148/radiol.2502080849
18. Rosenkrantz AB, Oei M, Babb JS, Niver BE, Taouli B. 2011. Diffusion-weighted imaging of the abdomen at 3.0 Tesla: image quality and apparent diffusion coefficient reproducibility compared with 1.5 Tesla. *J Magn Reson Imaging* 33(1): 128-135. https://doi.org/10.1002/jmri.22395
19. Ye XH, Gao JY, Yang ZH, Liu Y. 2014. Apparent diffusion coefficient reproducibility of the pancreas measured at different MR scanners using diffusion-weighted imaging. *J Magn Reson Imaging* 40(6): 1375-1381. https://doi.org/10.1002/jmri.24492
20. Bojorquez JZ, Bricq S, Acquitter C, Brunotte F, Walker PM, et al. 2017. What are normal relaxation times of tissues at 3 T? *Magn Reson Imaging* 35: 69-80. https://doi.org/10.1016/j.mri.2016.08.021
21. Hocaoglu E, Aksoy S, Akarsu C, Kones O, Inci E, et al. 2015. Evaluation of diffusion-weighted MR imaging in the diagnosis of mild acute pancreatitis. *Clin Imaging* 39(3): 463-467. https://doi.org/10.1016/j.clinimag.2014.10.001
22. Ma C, Pan CS, Zhang HG, Wang H, Wang J, et al. 2013. Diffusion-weighted MRI of the normal adult pancreas: the effect of age on apparent diffusion coefficient values. *Clin Radiol* 68(10): e532-e537. https://doi.org/10.1016/j.crad.2013.05.100

23. Yoshikawa T, Kawamitsu H, Mitchell DG, Ohno Y, Ku Y, et al. 2006. ADC measurement of abdominal organs and lesions using parallel imaging technique. *AJR Am J Roentgenol* 187(6): 1521-1530. https://doi.org/10.2214/AJR.05.0778

24. Herrmann J, Schoennagel BP, Roesch M, Busch JD, Derlin T, et al. 2013. Diffusion-weighted imaging of the healthy pancreas: ADC values are age and gender dependent. *J Magn Reson Imaging* 37(4): 886-891. https://doi.org/10.1002/jmri.23871

25. Schoennagel BP, Habermann CR, Roesch M, Hahne JD, Arndt C, et al. 2011. Diffusion-weighted imaging of the healthy pancreas: apparent diffusion coefficient values of the normal head, body, and tail calculated from different sets of b-values. *J Magn Reson Imaging* 34(4): 861-865. https://doi.org/10.1002/jmri.22743

26. Lemke A, Laun FB, Simon D, Stieltjes B, Schad LR. 2010. An *in vivo* verification of the intravoxel incoherent motion effect in diffusion-weighted imaging of the abdomen. *Magn Reson Med* 64(6): 1580-1585. https://doi.org/10.1002/mrm.22565

27. de Bazelaire CM, Duhamel GD, Rofsky NM, Alsop DC. 2004. MR imaging relaxation times of abdominal and pelvic tissues measured in vivo at 3.0 T: preliminary results. *Radiology* 230(3): 652-659. https://doi.org/10.1148/radiol.2303021331

28. Hoad CL, Cox EF, Gowland PA. 2010. Quantification of T(2) in the abdomen at 3.0 T using a T(2)-prepared balanced turbo field echo sequence. *Magn Reson Med* 63(2): 356-364. https://doi.org/10.1002/mrm.22203

29. Yoon SB, Choi MH, Lee IS, Lim CH, Kim JS, et al. 2017. Impact of body fat and muscle distribution on severity of acute pancreatitis. *Pancreatology* 17(2): 188-193. https://doi.org/10.1016/j.pan.2017.02.002

30. Li X, Zhuang L, Zhang X, Wang J, Chen T, et al. 2016. Preliminary study of MR diffusion tensor imaging of pancreas for the diagnosis of acute pancreatitis. *PLoS One* 11(9): e0160115. https://doi.org/10.1371/journal.pone.0160115

31. Nissan N, Golan T, Furman-Haran E, Apter S, Inbar Y, et al. 2014. Diffusion tensor magnetic resonance imaging of the pancreas. *PLoS One* 9(12): e115783. https://doi.org/10.1371/journal.pone.0115783